Denoising of Synthetic Aperture Radar Images Using Dual Tree Curved Wavelet Transform with Modified Cellular Neural Networks

Gouri S. Katageri and P. M. Shivakumara Swamy

Abstract Synthetic aperture radar, sometimes known simply as SAR, is a technique for imaging a target from space that uses microwave radiations to illuminate the object that is the focus of the picture. These brief bursts of microwave radiation are sent with the help of a piece of equipment known as RADAR. Denoising is an important pre-treatment step in image processing that has to be finished before an application-friendly picture can be produced. This step is necessary to create an image. They are versatile enough to be used for everything from digital photography to photographing satellites. Their range of applications is rather extensive. The imaging method known as synthetic aperture radar may be used in any weather, both during the day and at night, and it uses airborne radar to illuminate the earth's surface. Satellites inspired the development of this particular technology. Processing must first be performed on the recorded backscattered signals before synthetic aperture radar images can be produced using them. Because microwaves can travel through clouds and dirt, they are often used in settings where traditional imaging would be difficult. Speckle noise is a natural occurrence that may be observed as granular patterns in synthetic aperture radar images. These images are produced by synthetic aperture radar (SAR) technology. It could be difficult to eliminate speckles, a random multiplicative noise. Speckle is a sort of noise. Speckle is a kind of noise that occurs in coherent systems and is formed when echoes interact with transmitted signals. This interaction may result in either constructive or destructive interference. The appearance of the speckle lowers the overall image quality, which means that the application cannot use it since it is improper. Denoising SAR pictures is a tough approach, but it is important since there is noise in the images and it has to be removed. Denoising is a strategy that should be used to eliminate the noise, but all of the essential visual information should be preserved. Denoising may be done in either the spatial domain or the transform domain, both of which are acceptable choices. Combining the dual tree curved wavelet transform with modified cellular neural networks is said to produce a

G. S. Katageri (✉) · P. M. Shivakumara Swamy
JSS Academy of Technical Education, Bengaluru, India
e-mail: gouriskatageri@jssateb.ac.in

P. M. Shivakumara Swamy
e-mail: pmshivakumaraswamy@jssateb.ac.in

N. R. Shetty et al. (eds.), *Advances in Computing and Information*, Lecture Notes in Electrical Engineering 1104, https://doi.org/10.1007/978-981-99-7622-5_12

one-of-a-kind filter, which has both been hypothesized and produced as a possibility (DTCWT-MCNN). The recommended filter is implemented using SAR images and put through its paces to see how well it works. The recommended approach is given a score based on its efficacy, which is determined by utilizing objective metrics, and its performance is analysed to see how effectively it functions. Performance evaluation metrics such as Noise Mean Value (NMV), Mean Square Difference (MSD), Equal Number of Looks (ENL), Noise Standard Deviation (NSD), and Speckle Suppression Index were utilized to carry out quantitative confirmation of the findings. These metrics were utilized to confirm the findings (SSI).

Keywords Synthetic aperture radar · Denoising · Dual tree curved wavelet transform with modified cellular neural networks · Noise mean value (NMV) · Mean square difference (MSD) · Equal number of looks (ENL) · Noise standard deviation (NSD) · Speckle suppression index (SSI)

1 Introduction

Synthetic aperture radar, sometimes known simply as SAR, is a technique for imaging a target from space that uses microwave radiations to illuminate the object that is the focus of the picture. These brief bursts of microwave radiation are sent with the help of a piece of equipment known as RADAR. To generate SAR images, reflected echoes received from the target object are recorded, and the signals are then processed [1]. Because it is an inherent part of the photographs, the multiplicative speckle noise typical of SAR photos is notoriously eliminated. Speckle is a kind of noise that occurs in coherent systems and is formed when echoes interact with transmitted signals. This interaction may result in either constructive or destructive interference [2]. The appearance of the speckle lowers the overall image quality, which means that the application cannot make use of it since it is improper for the purpose. Removing specks from SAR photos is difficult, but it is required because of the need to do so. Despeckling is a method that is used for this purpose [3]. The removal of speckle noise from SAR images is the primary objective of this research, which uses a modified version of a method known as the wavelet transform. This chapter will begin with an explanation of the theory that underpins the development of SAR pictures and the uses for those images. After that, it talks about the speckle noise that could be present in SAR systems and the performance tests that might be used to evaluate how well despeckling is working.

1.1 SAR Image Representation

Doppler shift is a phenomenon that allows SAR to attain higher angular resolutions than it would otherwise be able to. SAR devices can capture the amplitude and

the phase of the signal being sent. In coherent systems, this phase information is preserved in its original state, making it feasible to put together signals captured in the past. The SAR systems keep the phase histories of the replies [4] at each location as the beam sweeps over the scene while simultaneously performing weighting, shifting, and summing operations to focus on a single target point. This is done simultaneously while the beam is scanning the image. After then, the image corresponding to the target's location is created.

Before the SAR image is made, the information about the dispersed target represented in two dimensions (range x azimuth), as shown in Fig. 1, is compressed. This may be seen in the Fig. 1. Convolving a range signal with a range reference will result in the production of data that has been compressed making use of range [5]. When it comes to azimuth compression, the convolution of the azimuth signal with the generated azimuth reference function is carried out in the frequency domain. In the same line as the previous sentence, as a consequence of this, the image that is constructed matches the target point's location. According to [6] the complexity of SAR images is becauseachixel contains both a real component and an imaginary component, also referred to as the amplitude and phase information, respectively. The link between beam width and phase is shown in Eq. 1, which may be found below.

$$\theta_{\text{ma}} = -\frac{4}{\pi} \cdot r + \phi_{\text{objec}} \tag{1}$$

The complex phasor representation of SAR images containing amplitude and phase is as in Eq. 2

Fig. 1 Example of SAR images

$$A \cdot \cos(2\pi f_a t + \phi) = A \cdot \text{Arp}[j(2\pi f_a f + \phi)]. \tag{2}$$

where 'A' gives the amplitude, 'f' is the frequency, and 'ϕ' is the phase.

1.2 SAR Image in Intensity Format

The intensity of SAR image denoted by G is related to the backscattering coefficient B which follows a multiplicative model given by Eq. 3.

$$G = BV \tag{3}$$

where V is the normalized fading random variable with unit mean and variance $1/L$ where L represents average number of images [7]. Here V follows a Gamma Distribution. Probability Density Function (PDF) of V is given by Eq. 4.

$$P_v(V) = \frac{L^{\perp} V^{L-1} e^{-LV}}{\Gamma(L)} \tag{4}$$

where $V \geq 0, L \geq 0$ and ${}^*\Gamma(-)^{\top}$ denote gamma function. Taking the bogarithmic transform converts the above equation into Eq. 5.

$$g = b + v \tag{5}$$

where $g = \ln(G), b = \ln(B), v = \ln(V)$.

The act of denoising an image is an essential step that creates the foundation for further developing and perfecting various ideas relating to image processing. The approach to remove the noise from the picture must be effective in computation and maintain aesthetically significant parts of the image, such as the image's edges and contours. The method of removing speckle noise from images is referred to as "despeckling," [8] and given that name as well. The use of image processing techniques such as averaging neighbouring pixels or spatial filtering may help reduce the appearance of speckle. Still, these techniques are unable to completely get rid of the problem. Multilooking is still another way, and it is the process of taking numerous separate images of the same location by applying different sections of synthetic aperture. This method is also known as "multilooking" which refers to the practise of "multilooking." On the other hand, these results in a decrease in the spatial resolutions that is accessible. They are added together and averaged to produce a more consistent picture. Utilizing a random variable as part of a statistical model of speckle noise is one of the approaches that may be taken to do this. When the data is presented in an intensity format, Reference [9] describes it as either a Gamma distribution or a multi-convolution of the Rayleigh probability density. However, when the data is presented in an amplitude format, Reference [10] describes it as a

multi-convolution of the Rayleigh probability density. Reference [11] most available noise models have been modified to be used with AWGN. The logarithmic transform is executed, and the additive form of the multiplicative noise model is derived from the multiplicative noise model. This is done so that the advantages offered by these models may be taken advantage of. Taking the logarithmic transform has the effect of entirely changing the speckle statistics since it is a nonlinear procedure. This is because the logarithmic transform is nonlinear. This demonstrates the need to use an efficient despeckling approach that can eliminate speckle noise while preserving edge features. The difficulty of the despeckling procedure is contributed to by the multiplicative and unpredictable qualities of speckle noise. Because it is impossible to correctly forecast the spectrum of speckle noise, the process of despeckling is rendered considerably more difficult than it would otherwise be.

The despeckling [12] procedure may be successfully carried out in either the transform or spatial domains. Both of these domains are valid possibilities. Transform domain techniques accomplish the elimination of speckle noise via the use of the thresholding of the transform coefficients as the method. When working in the spatial domain, a window or mask is moved over an image pixel by pixel, and the value of the central pixel is replaced with a value that is mathematically determined based on the values of the other pixels in the window. These methods use several of the performance metrics discussed in Sect. 1 to evaluate the influence of speckle noise. The SAR imaging technique captures high-resolution remote sensing photos from broad terrain areas. This is done to better analyse the landscape. SAR is a form of imaging that may be carried out through satellite at any time of day or night, regardless of the weather, and can investigate inaccessible areas of the globe's surface. SAR images are put to use for several different purposes, including navigation and guidance, the detection of snow wetness and glacier monitoring, the monitoring of foliage and ground penetration, the indication of moving targets, wave spectra, wind speed, ocean currents, change detection, and the monitoring of both the military and the environment. Speckle noise is a feature that is inherently present in SAR photographs and may be recognized in the image as granular patterns.

Reference [13] this noise can be observed in the image. Speckle is an effect that multiplies noise and also contains a random component, which makes the process of noise reduction more challenging. Speckle is a multiplicative effect. The appearance of speckle results in a loss in contrast, a change in the shape or size of the objects in the image, and a blurring of the borders between the various parts of the image. In addition, it magnifies the size of the picture's minute details. Most SAR despeckling algorithms complete the despeckling process in either the transform domain or the spatial domain [14]. The spatial domain is the more common of the two. When applying methods that include the transform domain, the noisy coefficients present in the images may be eliminated via thresholds.

The process of despeckling is carried out using spatial domain techniques, which use the pixels located close to the region being processed. These techniques may be used to eliminate the speckle noise in pictures; however, the technique performs poorly in maintaining the tiny details and edges in the images. The resolution of the SAR image and its general usefulness are decreased directly, making automated scene

segmentation and interpretation considerably more challenging. Therefore, there is a need for an efficient way of despeckling that can respond to discontinuities in the image while maintaining the key geometrical aspects, such as edges and contours. This is a problem since there are currently no methods to do this. In addition, the organization of the structure of the paper may be summed up as follows: In Sect. 2, an analysis of the prior study is offered. Section 3 explains the methodology and materials of the proposed work. Section 4 examines the experiments' results, and Sect. 5 provides a conclusion and some suggestions.

2 Literature Survey

Signals are subjected to transformations to gain more granular information about the signals. The transform coefficients are used for filtering purposes by the approaches that fall within the transform domain filtering category. Methods that are based on thresholds and methods that are based on statistical models are the two categories that may be used to classify the transform domain-based filtering strategies. The transform coefficients are assigned threshold values for noise reduction when using the threshold-based technique. If the magnitude of the coefficients is less than the threshold, then the threshold is set to zero; otherwise, it is left unchanged or hard/soft thresholding is performed. This approach is predicated on the observation that noise dominates the coefficients at smaller scales, while the larger coefficients provide information pertinent to the problem. The accuracy of this procedure might vary greatly depending on which threshold is used.

Despeckling [15] procedures based on statistical models need proper modelling coefficients. The following paragraphs will discuss the different transform-based SAR despeckling approaches. The approaches that belong to the transform domain use various transforms, including wavelet, ridgelet, curvelet, contourlet, surfacelet, shearlet, bandlet, and others.

A significant step forward was taken in multiresolution analysis with the development of the wavelet transform, abbreviated as WT. Denoising based on wavelets worked well for point singularities but was computationally inefficient for geometry aspects with line or surface singularities. Later, a discrete wavelet version was developed and presented, providing superior directional selectivity. The directional selectivity may be significantly improved by the 2D complex wavelets' ability to simultaneously provide up to six directional data. Reference [16] were the ones who first presented the ridgelet transform. The ridgelets are the most effective way to express singularities along straight lines. However, genuine pictures are characterized primarily by curvature and surface singularities. As a result, a novel concept was conceived, according to which the picture would first be partitioned, and then the ridgelet transform would be applied to each partition. The term "curvelet transform" has been given to this block-based ridgelet transformation. Reference [17] are two references to look at. The discretized constructions of curvelets known as contourlets were first developed to accommodate critical sampling.

Contourlets include discrete rectangular grids. The most important element of the contourlet system is the tree-structured directional filter bank. Reference [18] to make contourlet capable of accommodating additional directional characteristics. There is a mother shearlet function in [19]. It is necessary to conduct the operations of scaling, shearing, and translating operations on the mother wavelet to record the direction of singularities. The bandlet transform that [20] developed was predicated on adaptive methods, and it is applied to pictures with textures that go beyond C2-singularities. This technique had several flaws, the most notable of which were its difficultly in adapting to new circumstances and its complicated computational nature. Their paper [21] presented a Stationary Wavelet-domain Wiener (SWW) speckle filter that works in the wavelet domain. The discrete wavelet transform was improved using this technique, which was an updated version of the procedure. This technique makes the homogenous portions more even in texture while retaining the sharp scatterers and edges. It does not provide satisfactory results when applied to regions with varying terrain types.

To despeckle SAR pictures, [22] proposed a wavelet-based technique that used maximum a posterior (MAP) estimate. In this instance, the wavelet coefficients were modelled using a Generalized Gaussian (GG) distribution. The disadvantage of using this strategy is that the procedure is time demanding, and the edge details are not maintained as accurately as they should be. According to the amount of textural energy, the wavelet coefficients may be broken down into various degrees of heterogeneity. The amount of computing that was required by this approach was excessive. The authors [23] used a despeckling method for SAR pictures based on the undecimated discrete wavelet transform (UDWT), and then they added the directional bandlet transform. The bandlet coefficients underwent adaptive sigmoid thresholding so that they could be analysed. The great directional selectivity of this method, which aided in the process of retaining edges, was a benefit of this strategy.

Reference [24] suggested a SAR despeckling method that used un-supervised Fuzzy C-Mean (FCM) clustering in the second-generation Translation Invariant Bandlet Transform (TIBT) domain. This clustering method was used in the SAR despeckling method. The algorithm presented a calculating technique for the optimal clustering number and specifies the signal and noise in the clustering operation. In addition, the algorithm proposes a way for clustering data. The use of the fuzzy approach brings to a reduction in edge blurring. A wavelet-based technique with undecimated directional filter banks was suggested by Zhang et al. in 2009. In this step, the directional banks in the log-transformed picture are smoothed out using the mean shift method to generate a group of images orientated in a certain direction. The use of mean shift helps keep the edge features, but it does so at the expense of neglecting the subtleties of the texture. Reference [25] in this case, backtracking was accomplished by combining the denoised picture from before with the image that had been processed using curvelet denoising. This was an effective technique for SAR despeckling that maintained the image's crisp edges, but the result was blurring the image's textures.

Speckle noise is something that may be seen in SAR photos, and it lowers the overall image quality. The difficulty of despeckling is increased directly due to

speckle's random and additive nature. This study aims to develop an effective method for despeckling that can successfully remove speckle noise from the SAR picture without destroying its edges or other finely detailed characteristics. The despeckling process may be carried out either in the transform domain or the spatial domain using one of these ways. Although the procedures in the spatial domain are simpler than the techniques in the transform domain, these techniques tend to over smooth the portions of the picture with heterogeneity [26]. Speckle noise can be efficiently removed by using the transform domain approaches; however the effectiveness of these techniques is dependent on the threshold value that is utilized. The non-local approaches use the redundancy in the pixels to despeckle the image, but this results in a more difficult procedure overall. Each of these approaches has a unique set of benefits and drawbacks. Therefore, the best method for despeckling SAR photos would be to mix these several approaches. The wavelet transform is an example of one of these approaches; it is based on non-local means modelling and uses techniques from the transform domain in addition to filtering at different stages of its operation. The wavelet transform is a useful tool for analysing situations involving additive noise, however it is not useful for eliminating multiplicative noise. The multiplicative speckle noise that affects SAR pictures is difficult to filter and eliminate. In addition, the wavelet transform cannot adapt to the curved edges and discontinuities in SAR pictures. The speckle noise in the picture has to be eliminated, and the SAR version of the wavelet transform, which will do this while maintaining the image's edges and contours, needs to be constructed.

3 Methodology and Materials of Proposed Work

The data included in satellite photography is very useful for analysing landscapes, ocean regions, and changes in the atmosphere. The subfield of satellite image processing is emerging within digital image processing. Identifying objects in satellite photos is difficult because of the negative aspects present on the surface of satellite images, such as (1) a noisy environment, (2) insufficient contrast, and (3) insufficient sharpness. The visual quality of satellite pictures is entirely responsible for determining the degree of precision achieved in satellite image processing operations. However, satellite photos often have artefacts such as blurriness, noise, and a lack of contrast distribution. When an image enhancement method is used, the accuracy of object segmentation and identification tasks performed on satellite pictures is significantly improved. The present applications require the following image enhancement approaches of satellite image processing as they are extensively required to improve the output quality of the aim they are attempting to reach. Removing noise from satellite photos enhancing contrast and reducing blurring in satellite images enhancing contrast in satellite images reducing blurring in satellite images. The primary satellite image processing techniques that are now in use are only supported by a single algorithm that may be mapped to any of the upgrades above, which indicates that these algorithms are not universally applicable to all three of these enhancements. As

a result, the purpose of this study is to present a different strategy for making those above three upgrades in satellite photos in the direction of an energetic manner by using an integrated approach. The picture improvement tasks of denoising, contrast enhancement, and sharpness enhancement are all within the scope of the technology that has been presented as a solution. Therefore, the approach that has been suggested has been given the name of the universal algorithm, which refers to a single method that has been devised to address different problems.

"Energetic technique of satellite image improvement on denoising utilizing dual tree curved wavelet transform with modified cellular neural networks" is the suggested method.

The emergence of noise in satellite pictures is brought on by both the image transmission process and the instrument's aeging. Because of the presence of noise in the picture, both the output quality and the quality of the segmentation and recognition are reduced.

3.1 Dataset

Radar Satellite-1 (RISAT-1) Microwave Remote Sensing Satellite is equipped with a synthetic aperture radar (SAR) Payload that operates in C-band (5.35 GHz). This provides the capability to image surface characteristics at any time of day or night and in any weather. The dataset contains photos obtained by ICEYE using its scan mode and taken in the Gulf of Bothnia, located between the western coast of Finland and the eastern coast of Sweden. The first photograph was obtained on 25 February 2022, while the second image was obtained on 6 March 2022.

3.2 Stages of Denoising

Image denoising using DTCWT is suggested and discussed in more depth in this section. Images of a considerable size are made up of numerous bands' worth of data, each of which takes up a significant amount of storage space. When dealing with such huge images or datasets, picture denoising becomes more significant to lower the bandwidth requirements for transmission over a network and storage space. The wavelet transform is a useful tool for many different image processing applications, despite its drawbacks. On the other hand, complex wavelet transform can circumvent these restrictions. This research contribution shows an implementation of the dual tree complex wavelet transform using an arithmetic encoding approach. The dual tree complex wavelet transform, or DTCWT, pushes the wavelet coefficient closer to zero. When combined with thresholding, this provides more zeros, which results in a larger denoising ratio for an image that has been denoised while maintaining a decent quality picture. This approach that has been presented utilizes an arithmetic coding algorithm to increase the denoising ratio while denoising a picture or data.

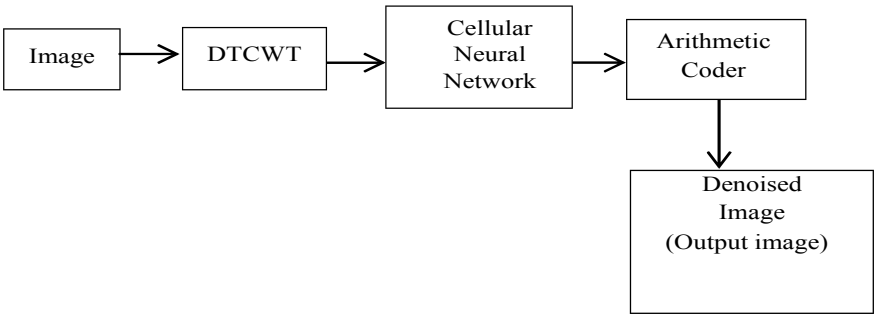

Fig. 2 Block diagram of DTCWT for image denoising

The block diagram of the proposed method is as given in Fig. 2.

To denoise the picture, a grayscale version is chosen. Initially, a dual tree complex wavelet transform is applied to the original picture, dissecting the image. The resulting coefficients are subjected to a threshold modification for further denoising using arithmetic encoding in the entropy process. Last but not least, the resulting compressed picture is used to calculate the denoising ratio.

4 Dual Tree Complex Wavelet Transform

This transform is a modification of the original DWT. The primary distinction between the DWT and the DTCWT comes from the fact that the DTCWT uses two filters, while the DWT only uses one. Figure 3 depicts these two filters, which together provide a result that contains twice as many wavelet coefficients as a signal with just one dimension. The complex wavelet coefficient is formed by the combination of these two tree coefficients, and its definition may be found in the following equations:

$$y_a + \mathrm{j}y_b \tag{6}$$

Or defined as in a polar form as

$$me^{j\theta} \tag{7}$$

In the above equation,'m' gives $\sqrt{y_a^2 + y_b^2}$ and $\theta = \tan^{-1}(y_b/y_a)$.

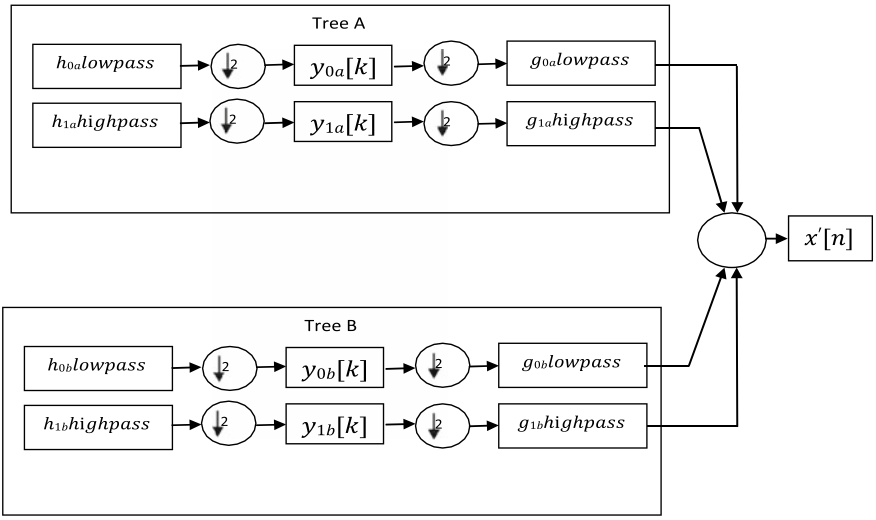

Fig. 3 Basic configuration of the dual tree filtering approach used to obtain the DTCWT coefficients

4.1 Dual Tree Framework

The DTCWT is based on the principle of deploying two actual DWTs, the first of which provides the real component, and the second of which provides the imaginary part.

Figure 4 illustrate how the implementation of the dual tree CWT is accomplished using the analysis and synthesis of FBs. To accomplish the perfect reconstruction using two separate real wavelet transforms, two distinct kinds of filters or sets of filters are used (PR). The combination of these two groups of filters results in the formation of an analytical transform. Upper FB and lower FB are the components that make up a filter pair.

For the upper FB, the low pass or high pass filter pair is represented by $h_0(n)$ and $h_1(n)$, whereas for the lower FB, the filter pair is denoted by $g_0(n)$ and $g_1(n)$, respectively. The filters were developed to meet the requirements of the PR condition, and as a result, the complex wavelet transform may be written as $(t) = h(t) + j(g)$ (this equation is in totally analytical form). To put it another way, they were developed in such a way that $g(t)$ is roughly equivalent to the Hilbert transform of $h(t)$.

Due to the fact that the filters themselves are actual, the implementation of DTCWT does not call for any complicated mathematical operations. Additionally, one more thing that should be brought to your attention is the fact that the DTCWT is not a critically sampled transform. Because the output data rate is precisely doubles that of the input data rate, it is exactly twice as costly as a signal that is just one dimension (1-D).

When compared to the forward transform, the inverse DTCWT is a very straightforward operation. In order to get two genuine signals, the inverse of each of the real

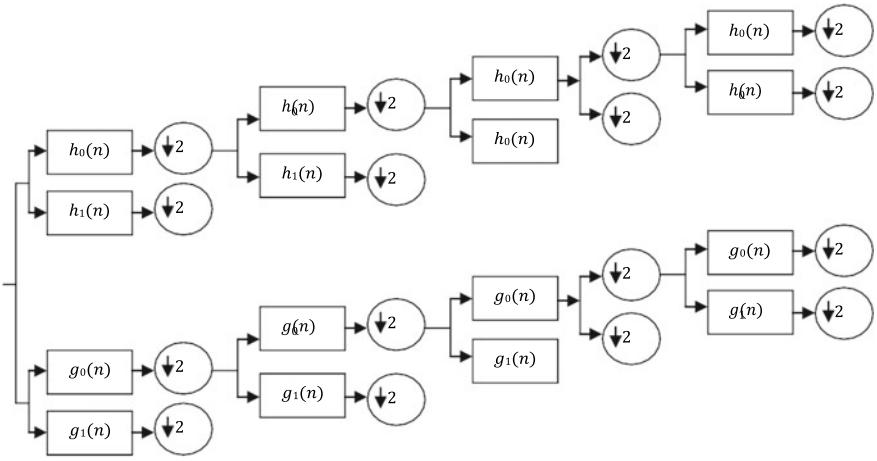

Fig. 4 Analysis filter bank for the dual tree discrete CWT

DWTs must be used. The final output is arrived at by taking the average of these two genuine signals.

In the event that a square matrix is employed to represent the two genuine DWT, a rectangle matrix will be used in order to depict the DTCWT:

$$R_n \text{ real part } R = [R_R \text{ imaginary pot}] \tag{8}$$

If the real signal is represented by the vector i, then the real part and imaginary part of DTCWT is denoted as

$$\begin{aligned} w_h &= R_h i; \text{ denotes the real part} \\ w_g &= R_g i; \text{ denotes the imaginary part} \end{aligned}$$

Then, the complex coefficient is given by the Equation:

$$w_h + j w_g \tag{9}$$

The inversion of Eq. (8) is given as:

$$\begin{aligned} R^{-1} &= \tfrac{1}{2}\left[R_h^{-1} R_g^{-1}\right] \\ R^{-1} \cdot R &= \tfrac{1}{2}\left[R_h^{-1} R_g^{-1}\right] \cdot \begin{bmatrix} R_h \\ R_g \end{bmatrix} \end{aligned} \tag{10}$$

The above Equation is used for the verification, i.e. $\frac{1}{2}[1+1] = 1$. As well as, the factor of one half between the forward and inverse transforms has to be shared to obtain.

$$R := \frac{1}{\sqrt{2}}\begin{bmatrix} R_h \\ R_g \end{bmatrix} \text{ and } R^{-1} = \frac{1}{\sqrt{2}}\left[R_h^{-1} R_g^{-1}\right]. \tag{11}$$

If the two real DWTs have an orthonormal relationship, then the inverse of R h and R g is the transpose of R h and R g. The left inverse may also be found in the transpose of a rectangular matrix. The DTCWT is defined by the Eq. (5.14), and this equation maintains the distinction between the real and imaginary parts of the CWT. On the other hand, complex coefficients are obtained by applying Eqs. 12 and 13, respectively.

$$\begin{aligned} R_c &:= \tfrac{1}{2}\begin{bmatrix} 1 & jI \\ 1 & -jI \end{bmatrix} \cdot \begin{bmatrix} R_h \\ R_g \end{bmatrix} \\ R_c^{-1} &= \tfrac{1}{2}\left[R_h^{-1} R_g^{-1}\right] \cdot \begin{bmatrix} I & I \\ -jI & jI \end{bmatrix}. \end{aligned} \tag{12}$$

Equation (5.15) gives the unitary,

$$\frac{1}{\sqrt{2}}\begin{bmatrix} I & jI \\ I & -jI \end{bmatrix} \cdot \frac{1}{\sqrt{2}}\begin{bmatrix} I & I \\ -jI & jI \end{bmatrix} = 1 \tag{13}$$

Algorithm 1 Image Despeckling()

Input: f(x, y) and Output: g(x, y)
Step 1: Read the input image and write in to DTCWT-MCNN description file as cells
Step 2: Then entire image of equivalent each cell that consists of the initial condition and/or input of the DTCWT-MCNN. The DTCWT-MCNN cells of cloning template are shown in Fig. 6(b) for edge detection
Step 3: After compiling the DTCWT-MCNN cell with the circuit description and image data using the pwl spice
Step 4: Then get the transient output of pwl spice
Step 5: Convert the pwl spice output data into binary data using BINF
Step 6: Finally, display the output image using PLOT with the binary output data

In point of fact, the Lyapunov function referred to above as $L(t)$ is just a function of the input intensity values vu(p, q) and the output intensity values vy(p, q) of the complete picture. Despite the fact that the state information does not provide all of the information on the variables vx(p, q). However, the steady-state characteristics of the state variables may be derived from the properties of the state variables that were derived from the properties of $L(t)$. It is possible to understand the Lyapunov function $L(t)$, which was described before, as the "generalized energy" of a DTCWT-MCNN. The subsequent adjustments will demonstrate that the strategy being offered converges and results in the best possible outcome. Figure 5 depicts the filter process that makes use of the improved DTCWT-MCNN algorithm.

Using the cloning templates, the instantaneous dynamic rules of DTCWT-MCNN are applied to each interaction.

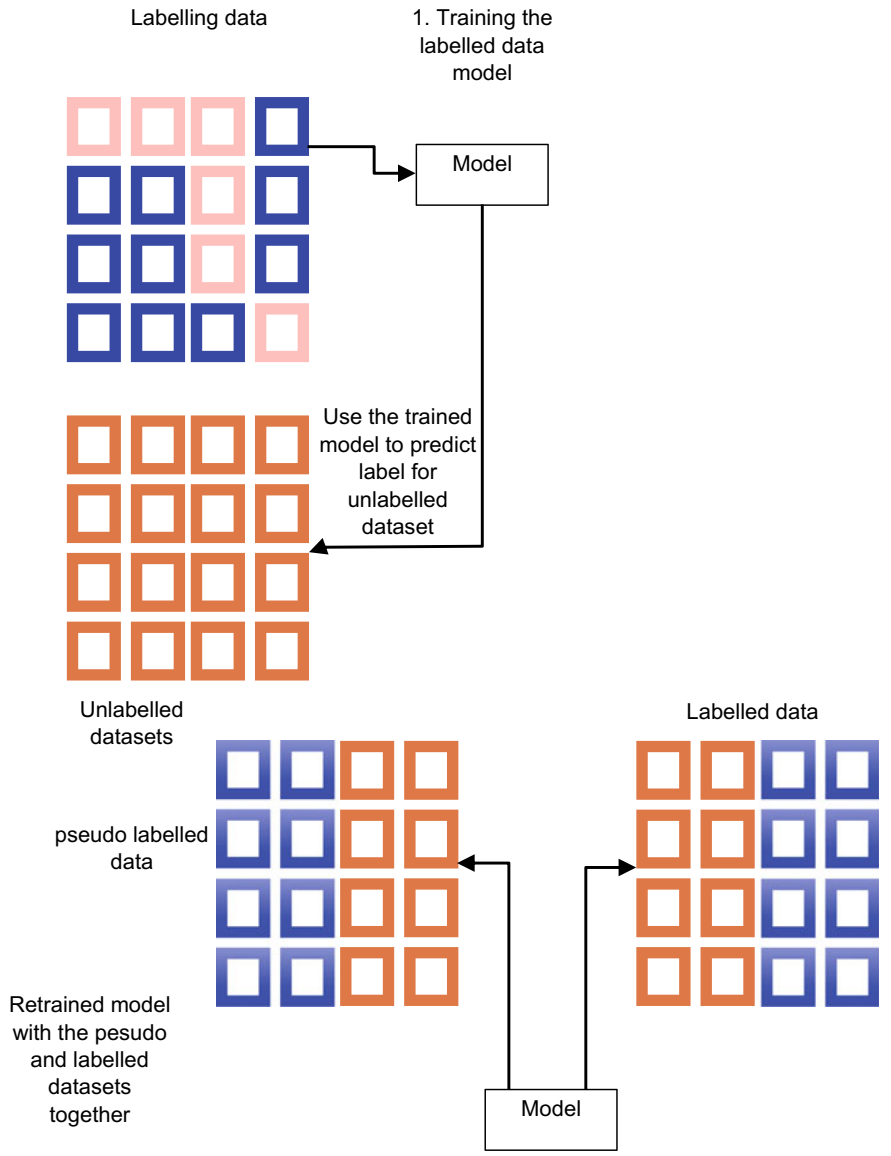

Fig. 5 Filtering operation using modified DTCWT-MCNN of size 3 × 3

5 Experimental Results

Matlab, version 9.8, an Intel i5 CPU, and the Windows 8.1 operating system are used to carry out the experimental examination of the suggested methodology in this section. The SAR satellite photos are intentionally messed up in order to acquire

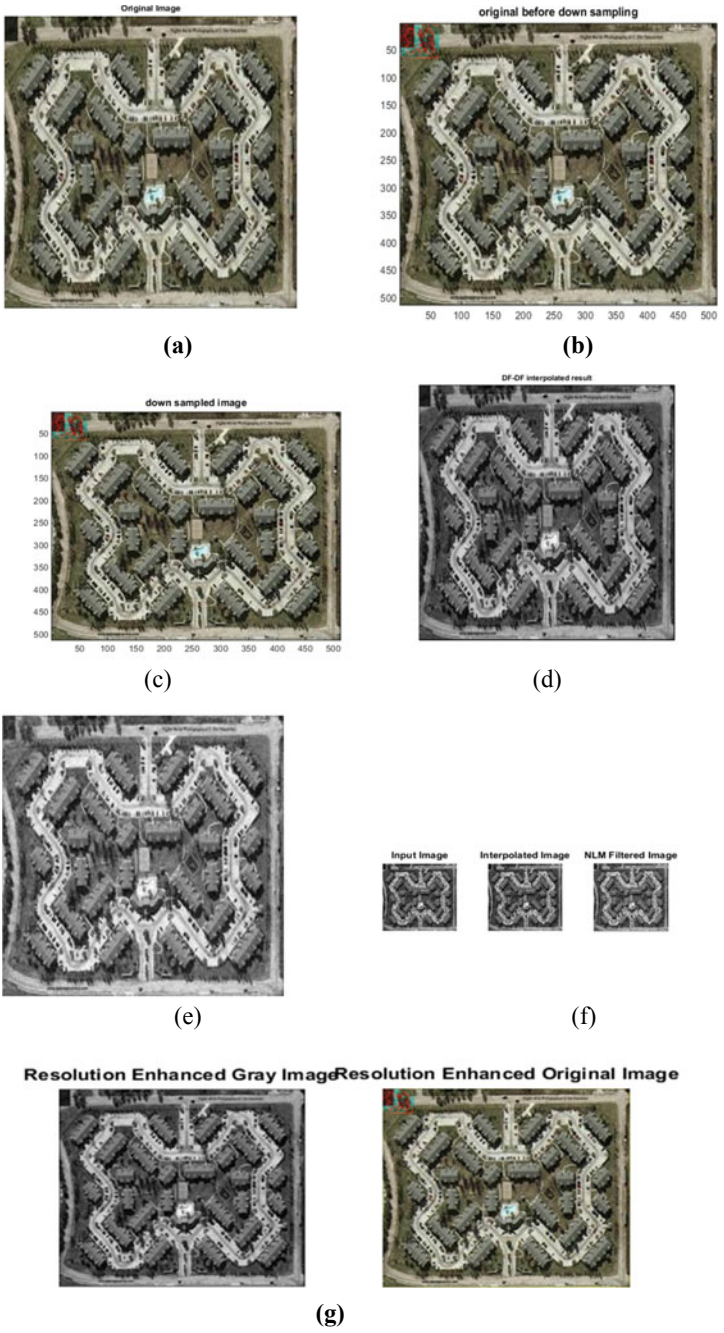

Fig. 6 **a** Input image, **b** down sampled image, **c** pre-processed image, **d** denoised image, **e** denoised image stage 2, **f** output image stage 1, and **g** output image stage 2

the training images. It is multiplied with each pixel of the original test picture by a random value that was created using the Rayleigh probability distribution with a mean of one so that the speckle noise effect may be analysed.

The following SAR photos were used for the validation process: ERS-1, Terra SAR-X, ASAR, Candian, C-SAR, and ERS-2. All of them are gathered from their respective places at different points over the earth's surfaces. The outcomes of the suggested method are contrasted with those of the already used methods by using measures such as the peak signal-to-noise ratio (PSNR), the root mean square error (RMSE), and the structural similarity index (SSI).

$$\mathrm{NSD} = \sqrt{\frac{\sum_{\min} (I_d(m,n) - NMV)^2}{M \times N}}$$

$$\mathrm{MSD} = \frac{\sum_m (I_x(m,n) - I_d(m,n))^2}{M \times N}$$

$$\mathrm{ENL} = \left[\frac{\mathrm{NMV}}{\mathrm{NSD}}\right]^2$$

$$\mathrm{SSI} = \frac{\sqrt{\mathrm{var}(I_d)}}{\mathrm{mean}(I_d)} \times \frac{\mathrm{mean}(I_x)}{\sqrt{\mathrm{var}(I_x)}}$$

where $I_d(m, n)$ is the despeckled image, M, N are the number of rows and columns of the image, respectively, and $I_s(m, n)$ is the speckled image.

The photos that were chosen for the experimental work are 512 by 512 pixels in size, and they were picked from fine- and medium-resolution photographs that had heterogeneous regions. The performance of the filler may be evaluated by first measuring the evaluation parameters on the whole picture, followed by measuring ENL and SS1 across uniform sections within the image. The value of k is determined by a process of trial and error. In order to accomplish the goals of the experiment, the scalar ($k = 2.5$) was chosen (Table 1).

The processing of the speckle noisy SAR pictures may provide results that are reflective of the experimental findings, which are shown in Figs. 6 and 7. These figures demonstrate the results acquired from the experiments. Figure 7 depiction of the findings demonstrates that the suggested method is superior to those now in use.

See Table 2 and Figs. 8, 9, 10, 11 and 12.

6 Conclusion

For the purpose of speckle reduction, a novel filtering strategy based on a modified DTCWT-MCNN has been developed. The process of filtering is carried out with the assistance of DTCWT-MCNN simulation as well as real-time SAR pictures. The spectral noise may be eliminated by using parallel processing and differential equations, as suggested in the technique. In this proposition, the power of

Table 1 Performance metrics of proposed work

Tested images	NSD	MSD	SSI	MSD
SAR Tiber Valley	2.2614	0.3278	1.2542	0.3014
SAR Maricopa	1.3307	0.4580	0.9452	0.4980
Canadian C-SAR	8.7611	5.2186	6.5142	3.0150
ASAR	8.8326	7.7278	6.9014	6.8124
ERS-2SARBuenos	7.6851	7.0154	6.3251	5.3289
Phonotom SAR	6.8515	6.0251	5.2490	3.2147
ERS-1SAR	8.2561	7.5314	6.2143	3.4501
SAR Volcano	8.9231	7.6321	6.0140	4.1483
ERS-2 SAR Coastal	7.5631	6.3214	5.1007	3.0016
Terra SAR-X	6.3153	5.6439	4.0198	3.5270

parallel processing offered by DTCWT-MCNN and Lyapunov's function are brought together. The experimental investigation of the suggested work is carried out, and the findings gained are compared with several ways that are already in use. It has been noticed that the recommended methods provide better outcomes than the methods that are currently being used. Because the results that have been achieved have been quite poor, it has been determined to improve the quality of the despeckled pictures by using rough set theory, which is excellent at making use of randomness and is superior in terms of approximation. In this study, an effort is made to get rid of speckle noise by using a proposed approach that is based on curvelets. The suggested method leads in a reduced quantity of speckle being present in the denoised picture, and the fine and medium-resolution images have better values of NMV than the low-resolution image does. Both the MSD and the ENL are buying at higher prices. It manifests itself as a higher decrease in speckle throughout the image's non-uniform and uniform portions. In addition to that, the performance is exceptional. The measure SSI has a value that is competent, which means it has less value than other metrics, which has the effect of reducing more speckle noise than other methods. Even in an environment with consistent conditions, the ENL and SSI values perform much better than the alternatives. As a direct consequence of this, the suggested technique is producing superior results numerically. Enhancing the characteristics that are already there in the picture results in an overall improvement to the image's quality.

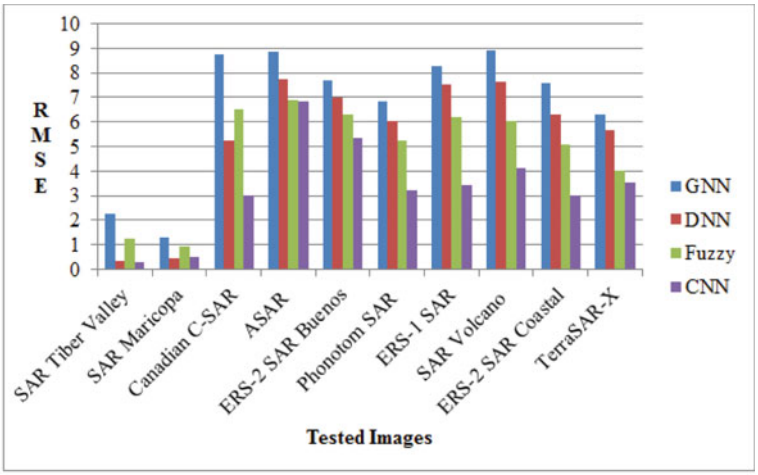

(a) Results of PSNR(dB)

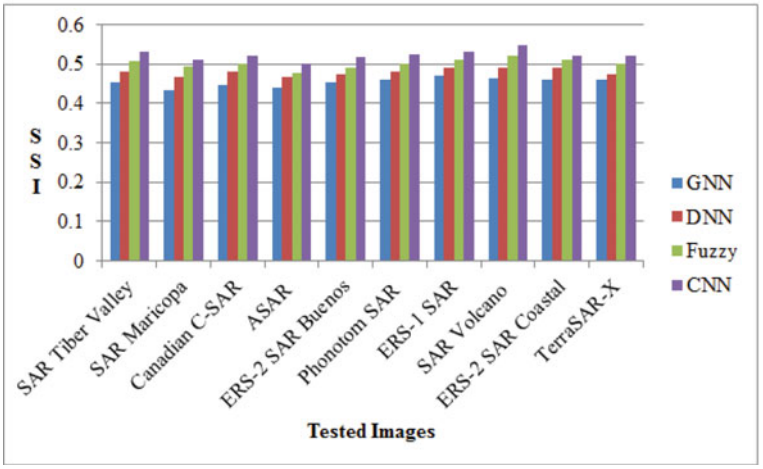

(b) Results of SSI

Fig. 7 Graphical representation of obtained results

Table 2 Performance metrics

Evaluation metrics	GNN	DNN	Fuzzy	Proposed
ENL	16.11	15.161	16.218	8.45
MSD	1712	1774	1774	0.551
NSD	68.79	58.84	60.31	0.238
NMV	118	117.23	118.71	0.695
SSI	162.10	157.28	162.83	182.46

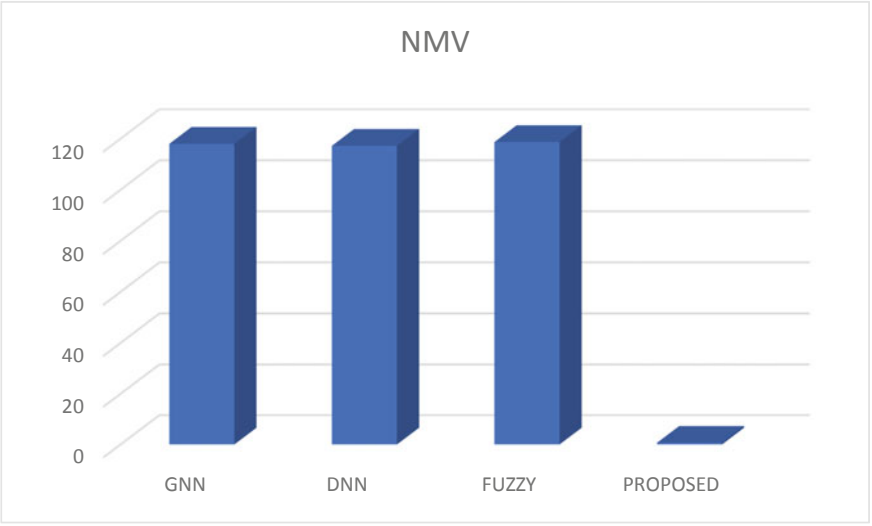

Fig. 8 Represents noise mean value (NMV)

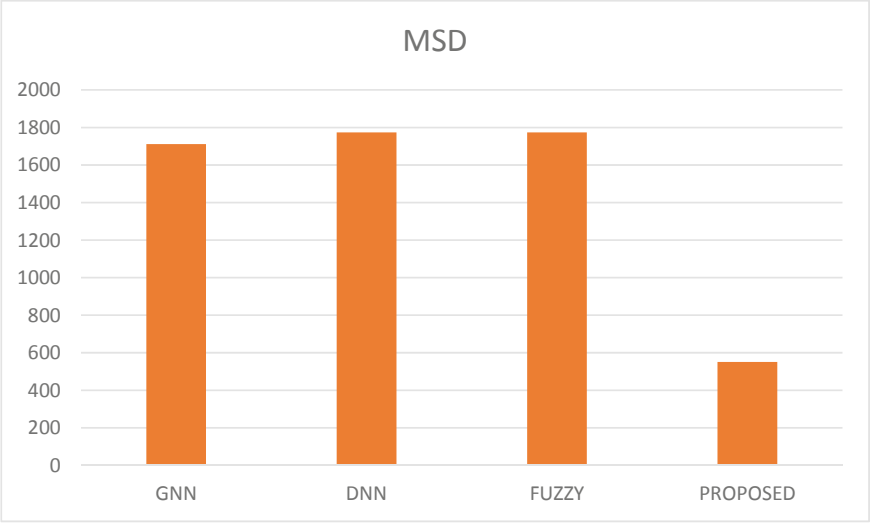

Fig. 9 Represents mean square difference (MSD)

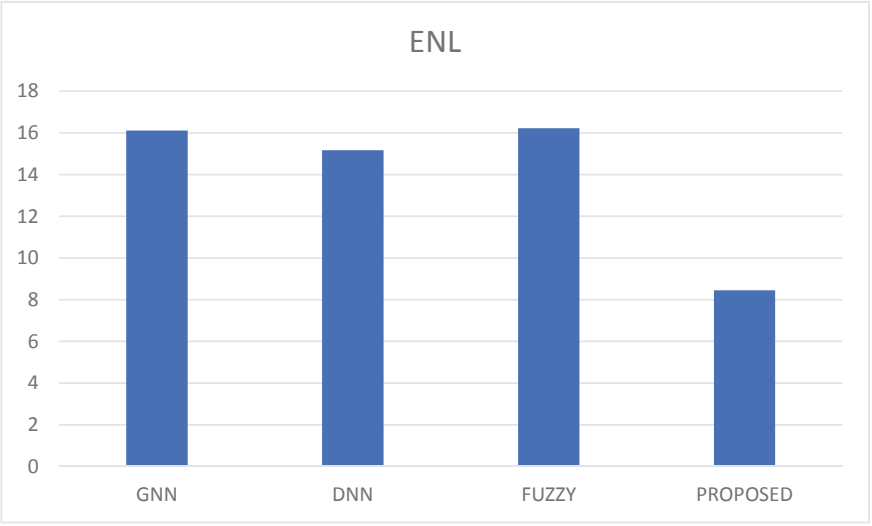

Fig. 10 Represents equal number of looks (ENL)

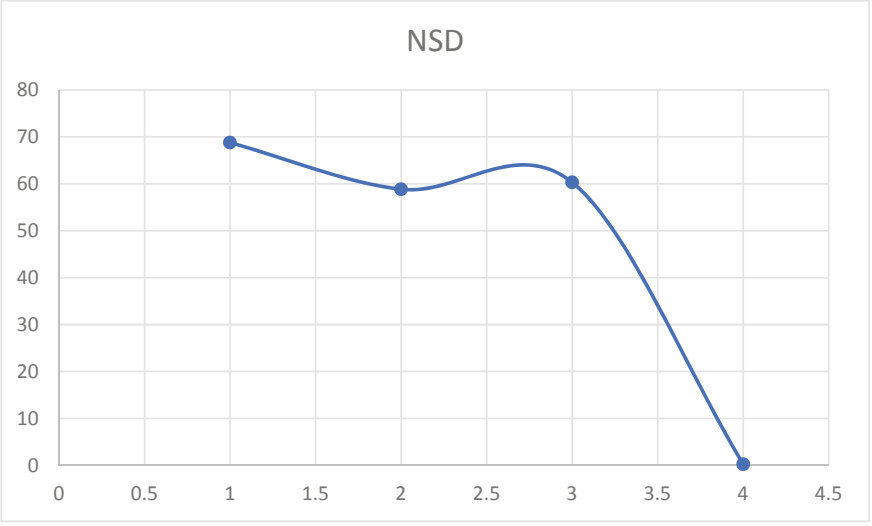

Fig. 11 Represents noise standard deviation (NSD)

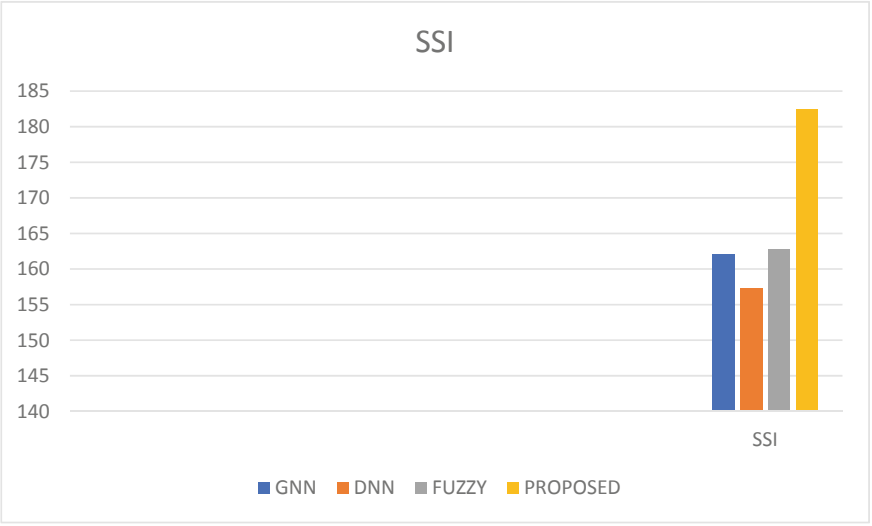

Fig. 12 Represents speckle suppression index (SSI)

References

1. Shuaiqi LIU, Yu LEI, Jiao PANG, Shuhuan ZHAO, Yonggang SU, Chenyang SUN. SAR image denoising based on generative adversarial networks. J Hebei Univ (Nat Sci Ed) 42(3):306
2. Huang Y, Sun G, Xing M (2022) A SAR image denoising method for target shadow tracking task. In: Proceedings of the 6th International conference on digital signal processing, pp 164–169
3. Huang H, Huang P, Liu X, Shao F, Li S, Lin X (2021) An iterative non-local denoising method of SAR image based on multi-resolution. In: 2021 7th Asia-Pacific conference on synthetic aperture radar (APSAR). IEEE, pp 1–5
4. Sun Y, Xin Z, Huang X, Wang Z, Xuan J (2021) Overview of SAR image denoising based on transform domain. In: 3D imaging technologies—multi-dimensional signal processing and deep learning. Springer, Singapore, pp 39–47
5. Parrilli S, Poderico M, Angelino CV, Verdoliva L (2011) A nonlocal SAR image denoising algorithm based on LLMMSE wavelet shrinkage. IEEE Trans Geosci Remote Sens 50(2):606–616
6. Achim A, Tsakalides P, Bezerianos A (2003) SAR image denoising via Bayesian wavelet shrinkage based on heavy-tailed modeling. IEEE Trans Geosci Remote Sens 41(8):1773–1784
7. Xu L, Li J, Shu Y, Peng J (2014) SAR image denoising via clustering-based principal component analysis. IEEE Trans Geosci Remote Sens 52(11):6858–6869
8. Liu S, Liu T, Gao L, Li H, Hu Q, Zhao J, Wang C (2019) Convolutional neural network and guided filtering for SAR image denoising. Remote Sensing 11(6):702
9. Parrilli S, Poderico M, Angelino CV, Scarpa G, Verdoliva L (2010) A nonlocal approach for SAR image denoising. In: 2010 IEEE International geoscience and remote sensing symposium. IEEE, pp 726–729
10. Gu F, Zhang H, Wang C (2020) A two-component deep learning network for SAR image denoising. IEEE Access 8:17792–17803
11. Subramanyam MV, Prasad G (2015) A new approach for SAR image denoising. Int J Electr Comput Eng 5(5)

12. Zhao J, Cao Z, Zhou M (2007) SAR image denoising based on wavelet-fractal analysis. J Syst Eng Electron 18(1):45–48
13. Schmitt A, Wessel B, Roth A (2009) Curvelet approach for SAR image denoising, structure enhancement, and change detection
14. Maji SK, Thakur RK, Yahia HM (2020) SAR image denoising based on multifractal feature analysis and TV regularisation. IET Image Proc 14(16):4158–4167
15. Cao X, Ji Y, Wang L, Ji B, Jiao L, Han J (2019) SAR image change detection based on deep denoising and CNN. IET Image Proc 13(9):1509–1515
16. Zhang Y, Ji K, Deng Z, Zhou S, Zou H (2016) Clustering-based SAR image denoising by sparse representation with KSVD. In: 2016 IEEE International geoscience and remote sensing symposium (IGARSS). IEEE, pp 5003–5006
17. Bai J, Hou B, Wang S, Jiao L (2008) SAR image denoising based on lifting direction let domain Gaussian scale mixtures model. Chin J Comput 31(7):1234–1241
18. Guofang S, Xin H, Licheng J (2003) SAR image denoising based on data fusion. In: Proceedings Fifth International conference on computational intelligence and multimedia applications. ICCIMA 2003. IEEE, pp 143–148
19. Abdullah HN, Hasan MF, Tawfeeq QS (2008) SAR image denoising based on dual tree complex wavelet transform. J Eng Appl Sci 3(7):587–590
20. Rezaei H, Karami A (2017) SAR image denoising using homomorphic and shearlet transforms. In: 2017 3rd International conference on pattern recognition and image analysis (IPRIA). IEEE, pp 80–83
21. Liu S, Hu Q, Li P, Zhao J, Zhu Z (2018) SAR image denoising based on patch ordering in nonsubsample shearlet domain. Turk J Electr Eng Comput Sci 26(4):1860–1870
22. Ponmani E, Saravanan P (2021) Image denoising and despeckling methods for SAR images to improve image enhancement performance: a survey. Multimedia Tools Appl 80(17):26547–26569
23. Zhao HH, Lopez Jr JF, Martinez A, Qiao ZJ (2013) SAR image denoising based on wavelet packet and median filter. In: Applied mechanics and materials, vol 333. Trans Tech Publications Ltd., pp 916–919
24. Yue C, Jiang W (2013) SAR image denoising in non sub-sampled contourlet transform domain based on maximum a posteriori and non-local constraint. Remote Sens Lett 4(3):270–278
25. Ji J, Li Y (2016) An improved SAR image denoising method based on bootstrap statistical estimation with ICA basis. Chin J Electron 25(4):786–792
26. Katageri GS, Shivakumara Swamy PM (2021) A novel model of SAR image edge enhancement and despeckling. In: 2021 International conference on forensics, analytics, big data, security (FABS). https://doi.org/10.1109/FABS52071.2021.9702546